

SPECT-Based Radiation Therapy and Transcatheter Arterial Chemoembolization for Unresectable Hepatocellular Carcinoma Sized 14 cm or Greater

Shintaro Shirai¹, Morio Sato¹, Yasutaka Noda¹, Kazushi Kishi¹, Akira Ikoma¹, Hiroki Sanda¹, Tetsuo Sonomura¹, Hiroki Minamiguchi¹, Motoki Nakai¹ & Nobuyuki Kawai¹

¹ Department of Radiology, Wakayama Medical University, Wakayama, Japan

Correspondence: Morio Sato, M.D. Department of Radiology, Wakayama Medical University, 811-1 Kimiidera, Wakayama Shi, Wakayama 641-8510, Japan. Tel: 81-73-441-0604. Fax: 81-73-444-3110. Email: morisato@mail.wakayama-med.ac.jp

Received: March 22, 2012 Accepted: April 5, 2012 Online Published: May 1, 2012

doi:10.5539/cco.v1n1p65

URL: <http://dx.doi.org/10.5539/cco.v1n1p65>

We have no sources of financial support and there are no financial disclosures from any authors

Conflicts of Interest: Actual or potential conflicts of interest do not exist

Abstract

Purpose: To evaluate the feasibility of single photon emission computed tomography-based three-dimensional conformal radiotherapy (SPECT-B3DCRT) combined with transcatheter arterial chemoembolization (TACE) for large unresectable hepatocellular carcinoma. **Methods:** Twelve patients with unresectable hepatocellular carcinoma (HCC) sized 14 cm or greater underwent SPECT using Tc-99m-galactosyl human serum albumin before 3DCRT to explore the optimal irradiation beam angle to cover the clinical target volume (CTV) to a total dose of 45 Gy/18 fractions while preserving functional liver volume (FLV). The TACE was scheduled within two months after completion of 3DCRT. **Results:** Local control rate was 78.6% at 2 years. Median over-all survival was 10.1 months and the survival rate at 1 and 2 years was 41.7 and 33.3%, respectively. **Conclusions:** SPECT-B3DCRT combined with TACE appears to be tolerable and effective for patients with HCC sized 14 cm or greater in terms of local control and survival.

Keywords: hepatocellular carcinoma, three-dimensional conformal radiotherapy, single photon emission computed tomography, functional liver

1. Introduction

Although this manuscript is mainly focused on single photon emission computed tomography-based three dimensional conformal radiation therapy (SPECT-B3DCRT), the idea of SPECT-B3DCRT arose originally to reinforce the efficacy of transcatheter arterial chemoembolization (TACE) for TACE-unmanageable hepatocellular carcinoma (HCC). TACE plays an important role in treating hepatocellular carcinoma (HCC) that is unresectable or unsuitable for radiofrequency ablation. However, TACE has two major limitations: it causes pathologically intensive liver infarction in patients with HCC invasion to the 1st branch and/or main trunk of the portal vein, resulting in poor prognosis; and local control in HCC sized 5 cm or greater is often difficult (R. Yamada et al., 1983) (Llovet et al., 2002) (Lo et al., 2002).

In these days, proton beam therapy is currently supplied for the uncontrollable HCC by TACE. Sugahara et al. reported that proton beam therapy accompanied with TACE for large HCC of 10–14 cm achieved an outcome, with 2-year survival of 36%, but proton beam therapy is not indicated for HCC 14 cm or greater (Sugahara et al., 2010). As the size of the HCC increases, wider beams are necessary to cover the whole tumor, resulting in the irradiation of cirrhotic liver surrounding the tumor. Liang et al. documented that the survival rate following three-dimensional conformal radiotherapy (3DCRT) worsens with increasing volume of HCC (Liang et al., 2005).

We attempted to use information obtained from single photon emission computed tomography (SPECT) with galactosyl human serum albumin (GSA) in conjunction with three-dimensional conformal radiation therapy (3DCRT) for unresectable HCC. Under the guidance of the SPECT image, the directions of two high-dose beams

were designed to cover the main tumor and portal vein tumor thrombus (PVTT), and to irradiate functional liver (FL) as little as possible. Our results showed that SPECT-based 3DCRT (SPECT-B3DCRT) did not cause radiation-induced liver disease (RILD), even in the presence of liver cirrhosis (Shirai et al., 2009). This safety was also assured for cases of HCC 8 cm or greater in maximum size (Shirai et al., 2010). Following these results, we attempted this radiation treatment for cases of HCC sized 14 cm or greater.

The purpose of the present study is to explore the safety and efficacy of combined therapy using SPECT-B3DCRT and TACE for HCC of 14 cm or greater, with cirrhotic liver, including Child–Pugh class B.

2. Materials and Methods

2.1 Patients and Tumor Characteristics

This prospective clinical investigation was approved by the Ethics Committee of our institute, and informed consent was obtained from all patients. The criteria for eligibility were as follows: (1) unresectable HCC; (2) giant HCC, or HCC with PVTT in the first branch or the main trunk, for which TACE is regarded to be ineffective or difficult because of the high risk of adverse effects; (3) the absence of extrahepatic metastasis; (4) no ascites, or under medical control of ascites; (5) Child–Pugh class A or B; and (6) performance status of between 0 and 2 on the Eastern Cooperative Oncology Group Scale. A total of 101 patients with HCC were enrolled between January 2005 and December 2009. Of these, we analyzed 12 cases of HCC with maximum diameter of 14 cm or greater on January 2011. The patient backgrounds and tumor characteristics are shown in Table 1. Based on the general rules of liver cancer study group of Japan (Liver Cancer Study Group of Japan, 2009), HCC was initially diagnosed on dynamic helical computed tomography (CT) or on dynamic magnetic resonance imaging using contrast medium. In 10 cases, tumor marker values of both α -fetoprotein (AFP) and proteins induced by vitamin K absence or antagonist-II (PIVKA-II) were elevated. The remaining two cases of HCC invasion to the portal vein and hepatic vein or intrahepatic bile duct showed PIVKA-II elevation alone. The HCCs were not surgically resected for the following reasons: advanced tumor stage with PVTT in the first branch and/or main trunk plus multiple intrahepatic metastases in 9 patients, and the prospect of insufficient residual liver volume for survival if surgical resection were conducted in 3 patients.

Table 1. Patient and tumor characteristics

Characteristics	Value
Total no. of patients	12
Age (yrs)	60 (53–87)
Gender	
Male	11
Female	1
Performance status	
0	5
1	5
2	2
Child–Pugh classification	
Class A	6
Class B	6
Surgical treatment	
Operable	0
Inoperable	12
Advanced tumor	9
Small residual liver volume for surgery	3
Hepatitis virus type	
HBV	3
HCV	4
Both	1
Unknown	4
Serum tumor marker level	
AFP (>20 ng/mL)	10
Median (range) (ng/mL)	4215 (52–76,544)
PIVKA-II (>40 mAU/mL)	12
Median (range) (mAU/mL)	4738 (97–302,680)
Tumor size in maximum diameter (cm)	17 (14–24)
No. of tumors	
Solitary	7
Multiple	5
Portal vein tumor thrombosis	
Present	9
Absent	3
AJCC stage	
T1N0M0, Stage I	3
T3N0M0, Stage III	9

TACE transarterial chemoembolization, *RT* radiotherapy, *HBV* hepatitis B virus, *HCV* hepatitis C virus, *AFP* alfa-fetoprotein, *PIVKA-II* proteins induced by vitamin K absence or antagonist-II, *AJCC* American Joint Committee on Cancer. Values are the number or median (range)

2.2 Identification of Functional Liver Volume

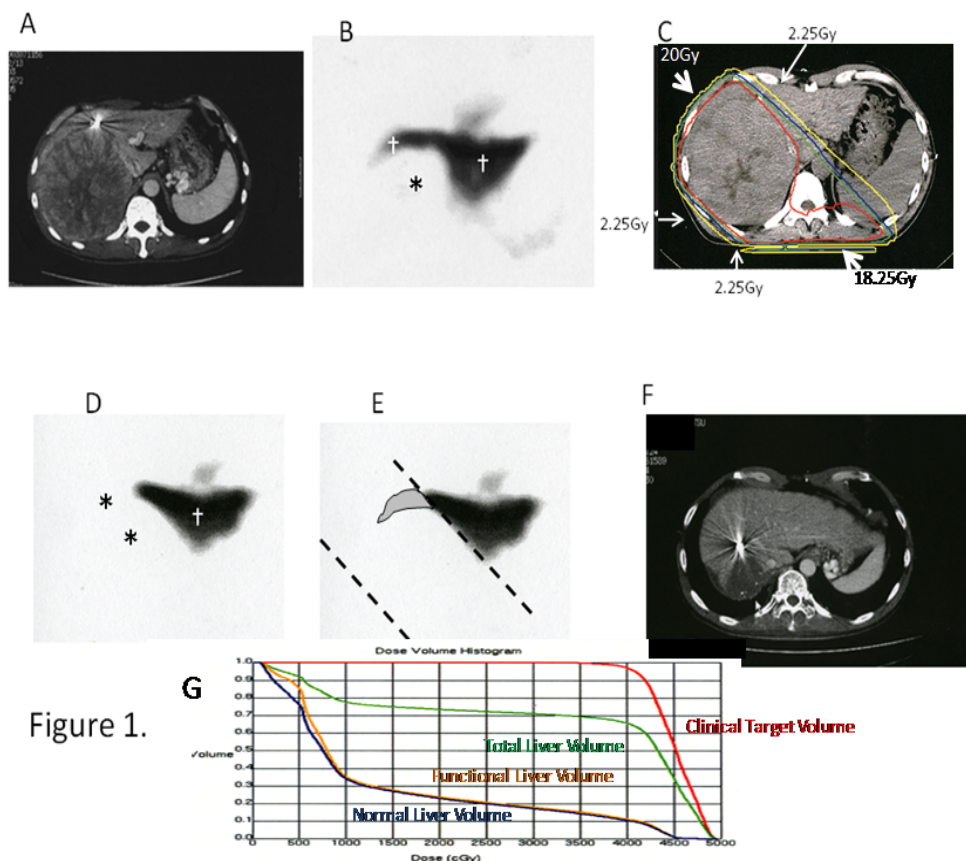
Functional liver was identified prior to radiation planning. SPECT images were acquired using Tc-99m-GSA (Nihon Medi-Physics, Tokyo, Japan) for functional imaging, and dynamic CT using contrast medium and simulation CT were performed within 2 weeks before commencement of 3DCRT. In each modality, whole liver images were obtained with 5 mm thickness for fine detail, during breath holding at end-expiration. Coincidence of the liver outline was used for reference. Normal liver (NL) was defined on dynamic CT as the area that remained after subtracting the HCC from the whole liver. The area of NL was then transferred to the SPECT images. Within NL, areas having the same hypo- or non-accumulation as HCC were defined as dysfunctional liver (DFL), and areas of hyper-accumulation compared with HCC were defined as FL. Information regarding HCC, FL, and DFL at each slice level was then transferred to the simulation CT images.

For the whole FL, the distribution ratio of functional liver volume (FLV) in the lobe with the clinical target volume (CTV) was termed the FLV distribution ratio and calculated as follows: FLV distribution ratio = FLV in the lobe with CTV/FLV in the whole liver \times 100 (%).

2.3 Destructive Functional Liver Volume (FLV) Ratio

2.3.1 Radiation Planning and Radiation Therapy

The SPECT-B3DCRT technique has been reported previously and is summarized briefly as follows (Shirai et al., 2009) (Shirai et al., 2010). Simulation CT was performed during breath holding. In order to control the respiratory movement, we let the patient practice to hold the breath at end-expiration under radio-fluoroscopic control in the simulation room. It is difficult to hold the breath during the irradiation of 2.5 Gy. Then, the patient was trained to hold breathing at end-expiration for 10-15 seconds at a time. Actually, the irradiation was repeatedly conducted for 10-15 seconds to reach to 2.5 Gy. Simulation CT was performed during breath holding. Simulation CT data were transferred to a 3DCRT planning system (Pinnacle, ADAC Labo, Milpitas, CA). Subsequent radiation planning is illustrated in Figure 1 and 2. The main tumor of maximum diameter 14 cm or greater and PVT was defined as the CTV. The planning target volume (PTV) included the CTV with a 10 mm margin to allow for respiratory-induced motion, and variations in daily setup.



Enhanced CT before RT (A) shows a giant tumor in the right lobe. SPECT before RT (B) shows a high-RI accumulation area corresponding to functional liver (†) and a non-RI accumulation area (*) corresponding to tumor. Dose distribution curves (from the innermost to outermost: 40, 30, 20, and 10 Gy, respectively) on simulation CT after radiation planning using high-dose (20 and 18.25 Gy) and low-dose (2.25 Gy) beams show the intensive irradiation to the giant tumor (C). SPECT obtained 2 months after completion of 3DCRT (D) shows an area of non-RI accumulation (*) corresponding to the two high-dose beams, with preservation of functional liver (†). Comparing (B) and (D), radiation-induced dysfunctional liver is shown as a gray area (E). One year after completion of RT, enhanced CT shows remarkable shrinkage of the giant tumor (F). Dose volume histograms of clinical target volume (CTV), total liver volume (TLV), normal liver volume (NLV) and functional liver volume (FLV) were shown in (G). *CT* computed tomography; *RT* radiotherapy;

SPECT single photon emission computed tomography; *RI* radioisotope; *3DCRT* three dimensional conformal radiotherapy

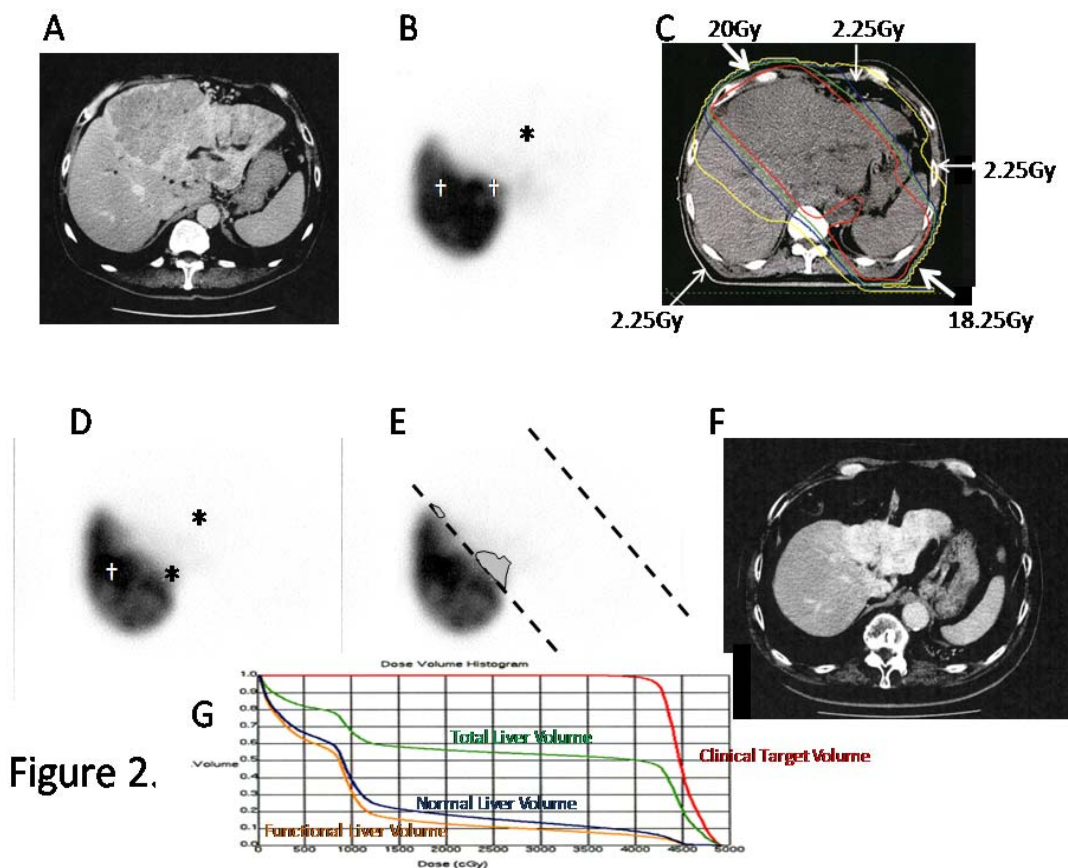


Figure 2.

Figure 2. A 58-year-old man with hepatocellular carcinoma 18.0 cm in maximum diameter

Enhanced CT before RT (A) shows a giant tumor in the left lobe. SPECT before RT (B) shows a high-RI accumulation area corresponding to functional liver (†) and a non-RI accumulation area (*) corresponding to tumor. Dose distribution curves (from the innermost to outermost: 40, 30, 20, and 10 Gy, respectively) on simulation CT after radiation planning using high-dose (20 and 18.25 Gy) and low-dose (2.25 Gy) beams show the intensive irradiation to the giant tumor (C). SPECT obtained 2 months after completion of 3DCRT (D) shows an area of non-RI accumulation (*) corresponding to the two high-dose beams, with preservation of functional liver (†). Comparing (B) and (D), radiation-induced dysfunctional liver is shown as a gray area (E). One year after completion of RT, enhanced CT shows remarkable shrinkage of the giant tumor (F). Dose volume histograms of clinical target volume (CTV), total liver volume (TLV), normal liver volume (NLV) and functional liver volume (FLV) were shown in (G). *CT* computed tomography; *RT* radiotherapy; *SPECT* single photon emission computed tomography; *RI* radioisotope; *3DCRT* three dimensional conformal radiotherapy

First, we prescribed mean dose of 45 Gy (2.5 Gy/fraction) for CTV and then, two high-dose or three low-dose beams were determined. The directions of two high-dose beams were first designed to cover the PTV, and to irradiate FL as little as possible. The doses of the high-dose beams were limited to 38.25 Gy/18 fractions/4 weeks to prevent adverse effects to the duodenum, spinal cord, and stomach (Figure 1c and 2c) (Emami et al., 1991) (Park et al., 2005). Three additional low-dose beams of 6.75 Gy/18 fractions/4 weeks were required to elevate the dose to the CTV, resulting in a total dose of 45 Gy (2.5 Gy/fraction) to the isocenter (Park et al., 2002). These low-dose beams were designed to avoid irradiating risk organs such as the stomach, duodenum, and spinal cord. Doses of 2.25 Gy for each additional beam do not cause liver damage even if the beams irradiate FL. In terms of the kidneys, the volume irradiated at 20 Gy or more was planned to not exceed 30% of the total volume. The couch angle was adjusted to the maximum limit of 90° to complete this planning.

2.3.2 Estimation of Radiation-Induced DFL Volume

We speculated that if RILD occurred, its occurrence would correlate with radiation-induced DFL volume (RIDFLV) (Shirai et al., 2010). Follow-up SPECT was obtained 2 months after completion of RT (Figure 1D and 2D) and was used to determine RIDFLV (Figure 1E and 2E) in comparison with the reference SPECT image obtained before RT (Figure 1B and 2B). We compared the image showing the iso-dose curves on the simulation CT with the SPECT image that obtained after 3DCRT (Figure 1C and 1D, 2C and 2D, respectively). RIDFLV was then contoured on the simulation CT with reference to the SPECT image that obtained before and after 3DCRT (Figure 1B and 1D, 2B and 2D). FLV was outlined on the simulation CT with reference to the CT and SPECT images before 3DCRT. The destructive ratio of RIDFLV versus FLV was defined as $\text{RIDFLV}/\text{FLV} \times 100$ (%).

The mean dose to normal liver (MDTNL) has previously been used as an indicator in RILD analysis (Xu et al., 2006); in the present study, we compared MDTNL with the mean dose to functional liver (MDTFL) (Shirai et al., 2010) by summing the dose values of all voxels within normal liver or functional liver and dividing this value by the number of voxels.

2.3.3 TACE and Follow-Up Evaluation

We planned combination treatment of RT and TACE for gigantic tumors with/without PVTT. SPECT-B3DCRT was performed initially, with follow-up SPECT and dynamic CT using contrast medium 2 months later for evaluation. Superselective TACE using 5–15 mL lipiodol (Guerbet, Charles de Gaulle, France) with or without gelatin sponge particles (Gelpart, Nihonkayaku, Tokyo, Japan) was performed within 2 months of completion of SPECT-B-3DCRT for main tumor, PVTT and tumor located outside the irradiated volume (Shirai et al., 2009) (Shirai et al., 2010). Main tumor plus PVTT were treated by the combination of SPECT-B-3DCRT and TACE. Further, repeat TACE was performed at follow-up if intrahepatic metastases or local progression of main tumor were detected.

Blood tests and liver function tests were conducted weekly during SPECT-B-3DCRT and monthly for 4 months, and several times before and after TACE. AFP and/or PIVKA-II tumor markers were measured every 1 to 3 months to evaluate tumor progression.

2.4 Evaluation of Toxicity

Adverse effects related to RT and TACE on skin, upper gastrointestinal tract, blood components, and liver were graded using the Common Terminology Criteria for Adverse Events v3.0 (CTCAE v3.0). Regarding adverse effects on the liver, RILD was defined as non-malignant ascites plus Grade 2 or worse non-icteric elevation of alkaline phosphate level (classic RILD) or elevation of transaminase level of Grade 3 or worse (non-classic RILD) (Xu et al., 2006). Further, we evaluated any deterioration in Child–Pugh score during the interval from 3DCRT finalization to TACE initiation. Yamada et al. documented a positive relation between a deterioration in Child–Pugh score and the percentage volume of the total liver that received a dose exceeding 30 Gy ($_{\text{TL}}V_{30\text{Gy}} \geq 40\%$) (K. Yamada et al., 2003). Then, we explored the values of $_{\text{TL}}V_{30\text{Gy}}$ and analyzed a relation between a deterioration in Child-Pugh score and FLV distribution ratio in the lobe with CTV (%) (FLVDR).

3. Statistical Analysis

We calculated the cumulative local control rate, progression-free survival (PFS), or overall survival from the day of commencement of 3D-CRT until the date of tumor progression within CTV; until the date of tumor progression contained within the CTV, intrahepatic metastases, or extrahepatic metastases; or until the date of death, respectively. We calculated the probability of local control, PFS, and overall survival according to the Kaplan–Meier estimator. Correlation between $\text{RIDFLV}/\text{FLV} \times 100$ (%) and FLV distribution ratio in the lobe with CTV was analyzed using Pearson's correlation analysis and Pearson's correlation coefficient.

MDTNL and MDTFL were compared in all patients using the paired t-test. The existence of toxicity was evaluated using Fisher's exact test. For each analysis, the statistical software package SPSS11.0J (SPSS Inc., Chicago, IL) was used and $p < 0.05$ was considered statistically significant.

4. Results

4.1 Tumor Progression and Survival after SPECT-B-3DCRT

Twelve cases of HCC sized 14 cm or greater were enrolled. The median follow-up period was 10.6 months (range, 2.2–42.5 months). At the last follow-up, 8 patients had died because of tumor growth and 4 patients have survived for 15.7, 20.6, 29.5 and 42.5 months. Patient background and tumor characteristics are listed in Table 1, and clinical progress is shown in Figure 3. New tumor progression within the CTV was detected during RT in one case (Case 2); following rupture of the HCC, treatment was discontinued and early death occurred at 2.2 months. Five cases (Cases 1, 3, 4, 8, 12) survived for more than 12 months, and three cases survived for more than 20 months.

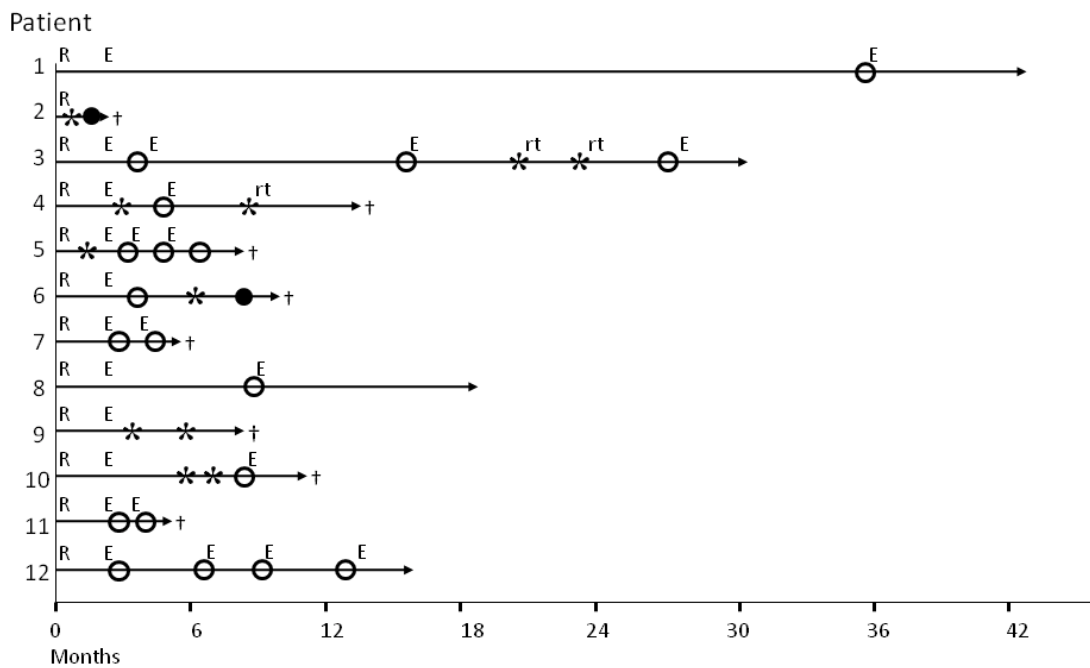


Figure 3. Clinical progress of 12 patients with HCC sized 14 cm or greater following SPECT-B3DCRT

RSPECT-B3DCRT; *E* transcatheter arterial chemoembolization; *rt* external beam radiation treatment for extrahepatic progression; *†* died; *•* local progression within CTV; *○* intrahepatic progression outside CTV; *** extrahepatic progression; *SPECT-B3DCRT* single photon emission computed tomography-based three dimensional conformal radiotherapy; *CTV* clinical target volume

Progression of the irradiated tumor (CTV failure) was observed in 2 cases (Cases 2, 6); the 1-, 2- and 3-year local control rates for the irradiated tumor were 78.6% (Figure 4). However, as shown in Figure 3, the intra-hepatic and/or extra-hepatic recurrences occurred, leading that progression free survival at 1 year, 2 year and 3 year was 8 %, 8 % and 0 %. The median survival time was 10.1 months; regarding overall survival, the 1-year survival rate was 41.7%, the 2- and 3-year survival rates were 33.3% (Figure 4).

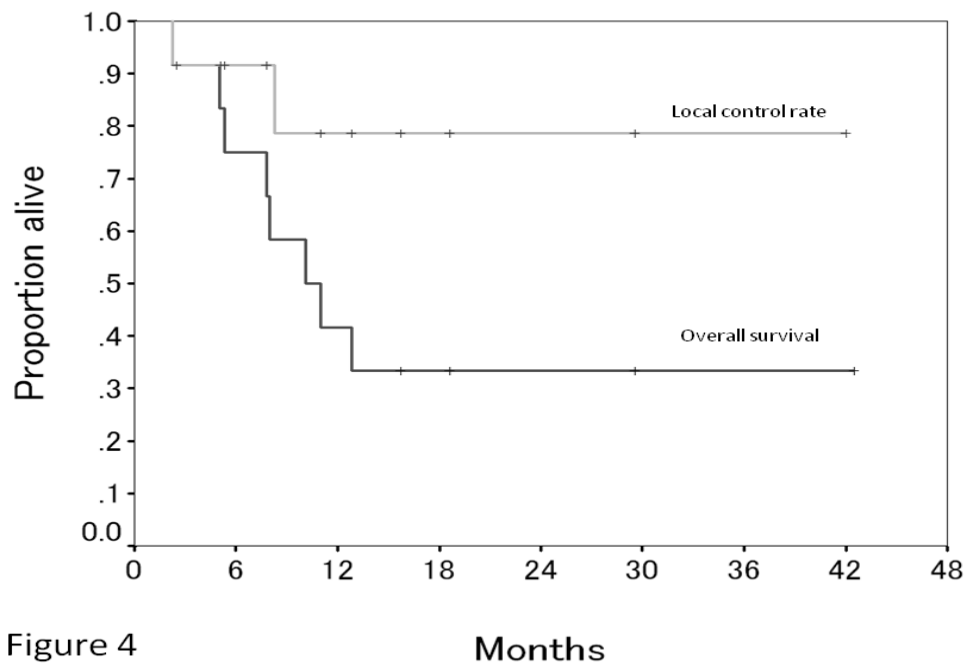


Figure 4. Kaplan-Meier analysis of the local control rate of the irradiated tumor (within clinical target volume) and overall survival in all 12 cases of HCC exceeding 14 cm following SPECT-B3DCRT. *HCC* hepatocellular carcinoma; *SPECT-B3DCRT* single photon emission computed tomography-based three dimensional conformal radiotherapy

4.2 Normal Liver Volume, Functional Liver Volume, and Clinical Target Volume

We analyzed correlations among NLV, FLV, and CTV (Table 2). The median CTV (1389 cm³) was greater than the median NLV (1154 cm³) in the whole liver. The FLV ratio (%) calculated using the value of FLV versus NLV in the whole liver, in the lobe with CTV (main tumor), and in the lobe outside CTV was 88 (64–99), 54 (0–97), and 98 (80–100), respectively, which indicates that nearly half of NL in the lobe with CTV was occupied by dysfunctional liver.

Table 2. Summary of dose–volume and functional–dysfunctional analysis

Variable	Range (median)
CTV (cm ³)	308–2535 (1389)
NLV (cm ³)	762–1976 (1154)
FLV (cm ³)	583–1779 (934)
FLV/NLV (%)	64–99 (88)
(FLV/NLV) in the lobe that includes CTV (%)	0–97 (54)
(FLV/NLV) in the lobe that does not include CTV (%)	80–100 (98)
FLV in the lobe that includes CTV/FLV in the whole liver (%)	0–27 (16)
FLV in the lobe that does not include CTV/FLV in the whole liver (%)	73–100 (84)
RIDFLV/FLV x 100(%)	4.4–27.4 (19.9)

CTV clinical target volume, *NLV* normal liver volume, *FLV* functional liver volume, *RIDFLV* radiation induced dysfunctional liver volume

4.3 Destructive Functional Liver Volume (RIDFLV) and Destructive Functional Liver Volume (FLV) Ratio

The FLV distribution ratio (%) was 16 (0–27) in the lobe with CTV and 84 (73–100) in the lobe outside CTV. In other words, most FLV existed in the lobes outside CTV. The MDTNL and MDTFL values of all patients were 1356 cGy (range, 1172–2126 cGy) and 1165 cGy (range, 915–1911 cGy), respectively. A significant difference existed between the doses to normal and functional liver ($p = 0.016$). The median and range of destructive FLV ratio (RIDFLV/FLV $\times 100$ (%)) by SPECT-B-3DCRT was 19.9 (4.4–27.4). Correlation analysis between FLV distribution ratio in the lobe with CTV and RIDFLV/FLV $\times 100$ (%) revealed a significant positive correlation (coefficient = 0.735, $p = 0.006$).

4.4 Toxicity

Toxicity based on CTCAE v3.0 after completion of 3DCRT is shown in Table 3. No patient fulfilled the definition of RILD. However, six cases experienced deterioration in Child–Pugh score. Of these, one (Case 2) was excluded because of progressive disease and the other five cases (Cases 3, 6, 9, 10 and 12) experienced a deterioration in score of 1. The median value of ${}_{TL}V_{30Gy}$ was 61 % (range, 40%–79%). In short, in each case the value of ${}_{TL}V_{30Gy}$ was $\geq 40\%$. Deterioration in Child–Pugh score (DCPS) was observed in five of the six cases with FLVDR $\geq 20\%$, but not in the five cases with FLVDR $< 20\%$ ($p=0.015$). FLVDR (%) of five cases with DCPS and six cases without DCPS was 21.8 ± 1.6 and 6.5 ± 10.5 ($p=0.015$), respectively.

Table 3. Therapy-related acute toxicity after completion of SPECT-B-3DCRT according to the Common Terminology Criteria for Adverse Events v3.0

Toxicity	Grade		
	1	2	3
Skin	4	0	0
Upper GI tract	3	0	0
Liver			
AST	1	0	0
ALT	0	0	0
ALP	1	0	0
Hematologic			
White blood cells	1	3	0
Platelets	2	1	1

SPECT-B-3DCRT single photon emission computed tomography-based three-dimensional conformal radiotherapy, *GI* gastrointestinal, *AST* aspartate aminotransferase, *ALT* alanine aminotransferase, *ALP* alkaline phosphatase

5. Discussion

As shown in Figure 1 and 2, two high-dose beams were planned to irradiate the large tumor, passing through the lobe with CTV (main tumor \pm PVTT) but reserving functional liver in the lobe outside CTV. It was necessary for these two beams to be wide enough to cover the full extent of the CTV, but it is clear that these beams would destroy functional liver in the lobe with CTV. In fact, a significant positive correlation was observed between the FL distribution ratio in the lobe with CTV and RIDFLV/FLV (%) (Coefficient = 0.735, $p = 0.006$). If these large HCC were surrounded by the lobe with the FLV, we would anticipate that the increase in RIDFLV/FLV (%) would induce RILD, as described by Liang et al (Liang et al., 2005). However, the median FLV ratios in the lobe with CTV and in the lobes without CTV were 54% and 98%, respectively. This finding indicates that approximately half of the NL in the lobe with CTV is occupied by DFL, whereas NL in the lobe outside CTV is occupied by FL. Moreover, the median FL distribution ratio in the lobe with CTV was low (16%), indicating that FL exists mainly in the lobe outside CTV. We consider that impairment of portal blood flow due to the compression of giant HCC and/or PVTT is the reason for the low FLV ratio and the low FL distribution ratio in the lobe with CTV.

MDTNL has been previously used as a safe indicator for predicting RILD (Xu et al., 2006). In the present study,

MDTFL was significantly lower than MDTNL, indicating that SPECT-B3DCRT contributes to reducing the radiation dose to functional liver. However, we previously described that neither MDTNL nor MDTFL contributed to predicting RILD (Shirai et al., 2010). In the present series, the maximum RIDFLV/FLV (%) was 27.4 % (Case 12; Figure 3), and we observed no evidence of RILD. Taking into consideration negative aspects associated with the present patients, such as maximum-sized HCC, 50.0 % frequency of Child–Pugh B liver cirrhosis, and 75.0 % frequency of PVTT, we consider that a value of RIDFLV/FLV (%) ≤ 27.4 % could indicate an upper limit that would protect against RILD. Yamada et al. indicated that $_{TL}V_{30Gy} \geq 40\%$ data were useful for predicting deterioration of liver function in their cases of HCC (K.Yamada et al., 2003); their data were not applicable to the present cases of gigantic HCC because in each case the value of $_{TL}V_{30Gy}$ was $\geq 40\%$, but FLVDR $\geq 20\%$ is considered a useful alternative.

It is difficult to control HCC sized 5 cm or greater using TACE alone. Lo et al. described HCC sized 5 cm or greater as an independent factor affecting local recurrence following TACE (Lo et al., 2002). Arata et al. described 56% (9/16) local progression-free survival for HCC greater than 5 cm following TACE + percutaneous ethanol injection therapy (Arata et al., 2001). In the present study, the total dose of 3DCRT for HCC of 14 cm or greater was 45 Gy (2.5 Gy/fraction) and TACE was scheduled to follow 3DCRT. The resulting 2-year local progression-free survival following SPECT-B-3DCRT plus TACE was 78.6 %. As shown in Figure 3, 11 of the 12 cases received not only SPECT-B-3DCRT but also TACE for main tumor and PVTT, and 9 cases did the further repeated TACE. The high local control rate was considered to be achieved with the assistance of TACE.

Liang et al. reported that all 12 patients with CTV greater than 1000 cm³ died within 20 months after 3DCRT (Liang et al., 2005). In the present study, 12 patients with the median CTV of 1389 cm³, the median overall survival time was 10.1 months and three cases survived more than 20 months.

A weakness of SPECT-B3DCRT is that the total irradiated dose to the CTV is limited because the liver is surrounded by the kidneys, duodenum, and spinal cord, which are radiation-sensitive. However, if we did not use GSA-SPECT for 3DCRT, the risk of RILD would rise, resulting in a reduction of over-all survival, as anticipated by Furuse et al (Furuse et al., 2005). Xu et al. reported that HCC patients with a mean hepatic CTV of 479.5 cm³ experienced RILD with a frequency of 15.6% following 3DCRT (Xu et al., 2006), and Cheng et al. reported that those with a mean hepatic CTV of 737–780 cm³ experienced RILD with a frequency of 17.65% (Cheng et al., 2002). In the present study, the median hepatic CTV was 1389 cm³ and no patient experienced RILD.

Stereotactic body radiation therapy (SBRT) is listed as a standard RT for HCC. However, Huang et al. 2011 documented HCC sized more than 4 cm was the independent poor prognostic factor and out-field intra-hepatic recurrence was the main cause of failure following SBRT for HCC. In this study, TACE was conducted for main tumor and PVTT, and out-field intra-hepatic recurrence, leading to the long survival. The contribution of repeated TACE accompanied with RT is considered to be crucial to control the out-field intra-hepatic recurrence.

The SPECT-B3DCRT is an on-going 3DCRT and a limitation exists that SPECT-B3DCRT is conducted under the voluntary breath-holding of the patient. Korreman S et al. 2011 reported that radiotherapy for lung cancer under four-dimensional computed tomography (4D-CT) provided a potential reduction of 37 % to 47 % in treatment field margins. The SPECT-B3DCRT for HCC under 4D image guidance might lessen the potential reduction. Another limitation is that the fusion of FLV is being conducted on the CE CT image with the use of the manual procedure in this study. Mechanical fusion of FLV to the normal liver with the use of SPECT-CT system reported by Hughes et al., 2012 would be preferable for SPECT-B3DCRT.

In conclusion, SPECT-B3DCRT with repeated TACE for new HCC tumors appears to provide safe irradiation of cirrhotic liver, achieving promising local control for HCC sized 14 cm or greater, and offering a better prognosis than other methods. Furthermore, FLVDR $\geq 20\%$ appears to be a predictive indicator for deterioration of liver function. However, a longer follow-up period and confirmation in a large study are required to evaluate these findings.

References

- Yamada, R., Sato, M., Kawabata, M., Nakatsuka, H., Nakamura, K., & Takashima, S. (1983). Hepatic artery embolization in 120 patients with unresectable hepatoma. *Radiology*, *148*, 397–401. <http://radiology.rsna.org/content/148/2/397.long>
- Llovet, J. M., Real, M. I., Montana, X., Planas, R., Coll, S., Aponte, J., & Bruix, J. (2002). Arterial embolisation or chemo-embolisation versus symptomatic treatment in patients with unresectable hepatocellular carcinoma: a randomized controlled trial. *Lancet*, *359*, 1734–1739. [http://dx.doi.org/10.1016/S0140-6736\(02\)08649X](http://dx.doi.org/10.1016/S0140-6736(02)08649X)
- Lo, C. M., Ngan, H., Tso, W. K., Liu, C. L., Lam, C. M., Poon, R. T., ... Wong, J. (2002). Randomized controlled trial of transarterial lipiodol chemoembolization for unresectable hepatocellular carcinoma. *Hepatology*, *35*, 1164–1171. <http://onlinelibrary.wiley.com/doi/10.1053/jhep.2002.33156/pdf>
- Sugahara, S., Oshiro, Y., Nakayama, H., Fukuda, K., Mizumoto, M., Abei, M., ... Tokuyue, K. (2010). Proton beam therapy for large hepatocellular carcinoma. *International Journal of Radiation Oncology Biology Physics*, *76*, 460–466. <http://dx.doi.org/10.1016/j.ijrobp.2009.02.030>
- Liang, S. X., Zhu, X. D., Lu, H. J., Pan, C. Y., Li, F. X., Huang, Q. F., ... Jiang, G. L. (2005). Hypofractionated three-dimensional conformal radiation therapy for primary liver carcinoma. *Cancer*, *103*, 2181–2188. <http://onlinelibrary.wiley.com/doi/10.1002/cncr.21012/pdf>
- Shirai, S., Sato, M., Suwa, K., Kishi, K., Shimono, C., Kawai, N., ... Nakai, M. (2009). Single photon emission computed tomography-based three-dimensional conformal radiotherapy for hepatocellular carcinoma with portal vein tumor thrombus. *International Journal of Radiation Oncology Biology Physics*, *73*, 824–831. <http://dx.doi.org/10.1016/j.ijrobp.2008.04.055>
- Shirai, S., Sato, M., Suwa, K., Kishi, K., Shimono, C., Sonomura, T., ... Nakai, M. (2010). Feasibility and efficacy of single photon emission computed tomography-based three-dimensional conformal radiotherapy for hepatocellular carcinoma 8 cm or more with portal vein tumor thrombus in combination with transcatheter arterial chemoembolization. *International Journal of Radiation Oncology Biology Physics*, *76*, 1037–1044. <http://dx.doi.org/10.1016/j.ijrobp.2009.03.023>
- Liver Cancer Study Group of Japan. (2009). *The general rules for the clinical and pathological study of primary liver cancer*. 5th ed. Tokyo: Liver Cancer Study Group of Japan.
- Emami, B., Lyman, J., Brown, A., Coia, L., Goitein, M., Munzenrider, J. E., ... Wesson, M. (1991). Tolerance of normal tissue to therapeutic irradiation. *International Journal of Radiation Oncology Biology Physics*, *21*, 109–122.
- Park, W., Lim, D. H., Paik, S. W., Koh, K. C., Choi, M. S., Park, C. K., ... Huh, S. J. (2005). Local radiotherapy for patients with unresectable hepatocellular carcinoma. *International Journal of Radiation Oncology Biology Physics*, *61*, 1143–1150. <http://dx.doi.org/10.1016/j.ijrobp.2004.08.028>
- Park, H. C., Seong, J., Han, K. H., Chon, C. Y., Moon, Y. M., & Suh, C. O. (2002). Dose-response relationship in local radiotherapy for hepatocellular carcinoma. *International Journal of Radiation Oncology Biology Physics*, *54*, 150–155. [http://dx.doi.org/10.1016/S0360-3016\(02\)02864-X](http://dx.doi.org/10.1016/S0360-3016(02)02864-X)
- Xu, Z. Y., Liang, S. X., Zhu, J., Zhu, X. D., Zhao, J. D., Lu, H. J., ... Jiang, G. L. (2006). Prediction of radiation-induced liver disease by Lyman normal-tissue complication probability model in three-dimensional conformal radiation therapy for primary liver carcinoma. *International Journal of Radiation Oncology Biology Physics*, *65*, 189–195. <http://dx.doi.org/10.1016/j.ijrobp.2005.11.034>
- Yamada, K., Izaki, K., Sugimoto, K., Mayahara, H., Morita, Y., Yoden, E., ... Sugimura, K. (2003). Prospective trial of combined transcatheter arterial chemoembolization and three dimensional conformal radiotherapy for portal vein tumor thrombus in patients with unresectable hepatocellular carcinoma. *International Journal of Radiation Oncology Biology Physics*, *57*, 113–119. [http://dx.doi.org/10.1016/S0360-3016\(03\)00434-6](http://dx.doi.org/10.1016/S0360-3016(03)00434-6)
- Arata, S., Tanaka, K., Okazaki, H., Kondo, M., Morimoto, M., Saito, S., ... Sekihara, H. (2001). Risk factors for recurrence of large HCC in patients treated by combined TAE and PEI. *Hepatogastroenterology*, *48*, 480–485.
- Furuse, J., Ishii, H., Nagase, M., Kawashima, M., Ogino, T., & Yoshino, M. (2005). Adverse hepatic events caused by radiotherapy for advanced hepatocellular carcinoma. *Journal of Gastroenterology and*

- Hepatology*, 20, 1512-1518. <http://onlinelibrary.wiley.com/doi/10.1111/j.1440-1746.2005.03916.x/pdf>
- Cheng, J. C. H., Wu, J. K., Huang, C. M., Liu, H. S., Huang, D. Y., Cheng, S. H., ... Huang, A. T. (2002). Radiation-induced liver disease after three-dimensional conformal radiotherapy for patients with hepatocellular carcinoma: Dosimetric analysis and implication. *International Journal of Radiation Oncology Biology Physics*, 54, 156-162. [http://dx.doi.org/10.1016/S0360-3016\(02\)02915-2](http://dx.doi.org/10.1016/S0360-3016(02)02915-2)
- Huang, W. Y., Jen, Y. M., Lee, M. S., Chang, L. P., Chen, C. M., Ko, K. H., ... Chang, Y. W. (2011). Stereotactic body radiation therapy in recurrent hepatocellular carcinoma. *International Journal of Radiation Oncology Biology Physics*, (in press). <http://dx.doi.org/10.1016/j.ijrobp.2011.11.058>
- Korreman, S., Persson, G., Nygaard, D., Brink, C., & Juhler-Nottrup, T. (2011). Respiration-correlated image guidance is the most important radiotherapy motion management strategy for most lung cancer patients. *International Journal of Radiation Oncology Biology Physics*, (in press). <http://dx.doi.org/10.1016/j.ijrobp.2011.09.010>
- Hughes, T., & Celler, A. (2012). A multivendor phantom study comparing the image quality produced from three state-of-the-art SPECT-CT systems. *Nuclear Medicine Communications*, (in press, 2012 Epub ahead of print). <http://dx.doi.org/10.1097/MNM.0b013e328351d549>